

## *Chapter 5*

### CONFORMATIONAL ANISOTROPY OF SIDE-GROUP LIQUID CRYSTAL POLYMERS IN NEMATIC LIQUID CRYSTAL SOLVENT: SMALL-ANGLE NEUTRON SCATTERING OF SEMIDILUTE SOLUTIONS

5.1 Introduction.....	123
5.2 Experimental.....	124
5.3 Results.....	125
5.4 Discussion.....	130
5.5 Conclusions.....	132
5.6 Tables.....	133
5.7 Figures.....	135
5.8 References.....	142

Rafael Verduzco contributed to the experiments discussed in this chapter. He synthesized and characterized the side-on polymers (names ending with “BB”). He and I traveled together to the NIST Center for Neutron Research (NCNR) where we shared the responsibility of performing the neutron scattering experiments. Zuleikha Kurji also assisted us with those experiments. We thank Boualem Hammouda and John Barker at the NCNR for their help with experimental design and interpretation of data.

## 5.1 Introduction

The molecules of a liquid crystal (LC) tend to align with one another in a preferred direction called the “director,” yielding a fluid material with anisotropic optical, electromagnetic, and mechanical properties. Random coil polymers are typically insoluble in LCs because of the entropic penalty to dissolution in an ordered solvent, but a side-group liquid crystal polymer (SGLCP) with mesogens covalently bonded to the polymer backbone can be dissolved in a small-molecule LC, where it adopts an anisotropic conformation as a result of its coupling to the orientational order of the host.<sup>[1-3]</sup> The shape of the polymer in solution depends on the thermodynamic balance between maximizing its conformational entropy and alignment of its side groups with the solvent’s nematic orientation field.

The coupling between the LC solvent and the polymer backbone is strongly influenced by the polymer architecture, the flexibility of the spacer connecting the side groups to the polymer backbone, and the strength of nematic interactions between the solvent and the side groups.<sup>[4]</sup> Attaching the side groups with their long axis perpendicular to the polymer backbone (“end-on”) usually causes the polymer to extend its conformation perpendicular to the director, but when side groups are attached with their long axis parallel to the backbone (“side-on”) the polymer tends to extend parallel to the director. The magnitude of the anisotropy is dependent on the flexibility of the spacer: when the side groups are connected by a rigid spacer their orientation is translated more efficiently to the polymer, but a flexible spacer provides partial screening of the orientational order. The anisotropy also depends on the strength of nematic interactions between the solvent and the side groups. When the pairwise interactions between the solvent and the side-groups are strong, the dissolved polymer strengthens the nematic order and when they are weak the solute polymer destabilizes the nematic phase.<sup>[5]</sup>

Small-angle neutron scattering (SANS) is an ideal tool for measuring the conformational anisotropy of SGLCPs. Anisotropic scattering patterns from samples with the nematic director aligned into a uniform, homogeneous monodomain allow the polymer’s dimensions to be probed in the directions parallel and perpendicular to the director. SANS

experiments are usually performed on dilute solutions of polymers to extract the dimensions of individual polymer chains. The experiments presented here are on solutions in the semidilute regime where the scattering from individual chains cannot be isolated. Although the polymers' sizes cannot be measured, their conformational anisotropy is readily accessible through measurement of the correlation length, the length beyond which a monomer's local environment contains monomers from other chains.

SANS experiments are performed on semidilute solutions of SGLCPs in a nematic solvent. The conformational anisotropy of closely matched end-on and side-on polymers is examined as a function of temperature and molecular weight, and comparisons between the polymers give insight into the coupling between configurational entropy and orientational order.

## 5.2 Experimental

### 5.2.1 Materials

Polybutadiene prepolymers were purchased from Polymer Source (Montreal, Quebec) and functionalized with end-on (SiCB4) and side-on (SiBB) mesogens to make side-group liquid crystal polymers (SGLCPs) (Figure 5.1). End-on polymers were synthesized according to the methods described in Appendix A and side-on polymers were synthesized by Rafael Verduzco.<sup>[6]</sup> The prepolymers had molecular weights of 48 kg/mol and 104 kg/mol and the characteristics of the converted SGLCPs are summarized in Table 5.1. The details of end-on polymer characterization may be found in Appendix A.

Perdeuterated 4-pentyl-4'-cyanobiphenyl ( $d_{19}$ 5CB, Figure 5.1) was synthesized according to methods described in Appendix B and had a nematic-to-isotropic transition temperature ( $T_{NI}$ ) of 32.3 °C. Solutions of 5 wt % SGLCP in  $d_{19}$ 5CB were prepared by dissolving the two components together in dichloromethane (DCM) then evaporating the DCM under an air stream followed by drying in vacuum overnight. The  $T_{NI}$ s of SGLCP solutions were within 1 °C of pure  $d_{19}$ 5CB's  $T_{NI}$ .

### 5.2.2 Small-Angle Neutron Scattering (SANS)

Cells were prepared by coating quartz plates with a rubbed polyimide alignment layer, then using epoxy to glue the plates together separated by an 813  $\mu\text{m}$  thick aluminum spacer ring. SGLCP solutions were loaded into the cells with a syringe. Cells were then placed in a room-temperature vacuum oven to remove small air bubbles and allowed to sit undisturbed for at least 18 hours prior to starting an experiment. This allowed enough time for the sample to align into a uniform monodomain under the influence of the alignment layers with the LC director parallel to the cell surfaces.

Small-angle neutron scattering (SANS) experiments were performed on the NG7 beamline at the National Institute of Standards and Technology Center for Neutron Research (NCNR). Cells containing homogeneously aligned SGLCP solutions were mounted in the beam contained in a temperature-regulated aluminum block held between the pole pieces of a 1.3 T electromagnet. The magnetic field served to reinforce the planar alignment induced by the rubbed polyimide layers and the neutron beam was incident perpendicular to the LC director. Samples were annealed at the desired temperature for fifteen minutes prior to collecting data. Experiments were performed at two temperatures in the nematic phase, 25 and 30  $^{\circ}\text{C}$ , and one temperature in the isotropic phase, 50  $^{\circ}\text{C}$ .

Two-dimensional scattering patterns were sector-averaged for easier visualization. Data having the same magnitude of the scattering vector,  $|\mathbf{q}| = q = 4\pi/\lambda \sin(\theta/2)$ , within  $\pm 15^{\circ}$  of the horizontal direction were averaged to give the scattering parallel to the director,  $I_{\text{par}}$ , and data in a sector of  $\pm 15^{\circ}$  from the vertical direction were averaged to give the scattering perpendicular to the director,  $I_{\text{perp}}$ .

## 5.3 Results

### 5.3.1 Conformational Anisotropy: Effects of Polymer Architecture, Temperature, and Molecular Weight

The scattering patterns from SGLCP solutions are anisotropic below the nematic-isotropic transition temperature ( $T_{NI}$ ) (Figure 5.2a,b) indicating that SGLCPs adopt ellipsoidal

conformations in LC solvent. These patterns are similar to other scattering patterns of SGLCPs in LC solvents reported in the literature<sup>[1-3]</sup> and similar to SANS patterns collected at Argonne National Laboratory's Intense Pulsed Neutron Source from polymers of identical structure, but different molecular weight.<sup>[7]</sup> Since the nematic director must be an axis of symmetry for the ellipsoid, it is deduced that end-on polymers adopt an oblate conformation while side-on polymers adopt a prolate conformation. A rough measure of the conformational anisotropy may be obtained from contours of equal scattered intensity on the two-dimensional patterns; the ratio of the major axis to the minor axis gives an aspect ratio. Thus calculated, the aspect ratios at 25 °C of side-on polymers 500HSiBB and 990HSiBB are 4.5 and 4.1, respectively, while end-on polymers 350HSiCB4 and 760HSiCB4 have aspect ratios at 25 °C of 1.6 and 1.7, respectively. In isotropic solvent, the scattering patterns from both end-on and side-on polymers are circularly symmetric (aspect ratio equal to one), indicating that polymer conformations are spherical (Figure 5.2c).

Conformational anisotropy is also evident in the polymers' sector-averaged scattering patterns (Figure 5.3-Figure 5.6). In the highest decade of  $q$ , side-on polymers scatter more strongly in the direction perpendicular to the nematic director (Figure 5.3 and Figure 5.4), while end-on polymers scatter more strongly in the direction parallel to the director (Figure 5.5 and Figure 5.6). Another rough measure of the anisotropy can be obtained from the ratio of the scattered intensity in the two orientations,  $I_{par}$  and  $I_{perp}$ , in the high  $q$  regime where  $I_{par}$  and  $I_{perp}$  are almost parallel. Measured this way at 25 °C, the side-on polymers, 500HSiBB and 990HSiBB, both have anisotropies  $I_{perp} / I_{par} \approx 10$  and the end-on polymers, 350HSiCB4 and 760HSiCB4, both have  $I_{par} / I_{perp} \approx 2$ .

Changing the molecular weight has very little effect on scattering patterns from 5 wt % solutions of side-on or end-on SGLCPs, suggesting that the polymer solutions are in the semidilute concentration regime.<sup>[8]</sup> End-on polymers are particularly insensitive to molecular weight; the scattering patterns from 350HSiCB4 and 760HSiCB4 are virtually superimposable on one another (Figure 5.5 and Figure 5.6). The scattering patterns from side-on polymers, 500HSiBB and 990HSiBB, also overlap one another at 25 °C, but when

the temperature is increased to 30 °C,  $I_{par}$  from 5 wt % 500HSiBB increases, indicating a decrease in the polymer's anisotropy (Figure 5.3). The anisotropy of 990HSiBB also decreases when the temperature is raised, but to a much lesser extent (Figure 5.4).

Scattering from all four polymer solutions is anomalously high at low  $q$ . Theoretically, the scattering from a solution of Gaussian polymer chains is described by the Debye equation,<sup>[9]</sup> which predicts the scattered intensity to become virtually independent of  $q$  as  $q$  approaches zero. The SGLCP solutions closely resemble the  $I \sim q^{-2}$  scaling predicted by the Debye equation at high  $q$ , and in an intermediate range all but  $I_{par}$  from side-on polymers begin to flatten out as predicted. However, strong deviations from the Debye prediction are observed at low  $q$  where the intensity takes a sharp upturn. Similar excess scattering at low  $q$  has been previously observed in semidilute solutions of poly(ethylene oxide) and attributed to associations between polymer chains.<sup>[10, 11]</sup> Supramolecular polymer aggregates have been observed in solutions of SGLCPs in isotropic solvents, such as tetrahydrofuran or chloroform, by light scattering<sup>[12-15]</sup> and rheology<sup>[16]</sup> and are attributed to specific interactions between the side groups of different polymer chains. The observation of inter-polymer associations confirms that solutions are in the semidilute regime.

In all four polymer solutions, the scattering patterns from isotropic solutions at  $T = 50$  °C have high- $q$  intensities intermediate between  $I_{par}$  and  $I_{perp}$  in the nematic phase (Figure 5.3-Figure 5.6). Otherwise, the patterns' qualitative shapes are not very different from nematic solutions.

### 5.3.2 Quantitative Analysis of Conformational Anisotropy: Fitting Data to Models

Models for dilute solutions of non-interacting polymer chains, such as the Debye equation, cannot be applied to the data from SGLCP solutions. Instead, the data are fit to the form

$$I(q) = \frac{C_1}{q^n} + \frac{C_2}{1 + (qL)^m} + C_3. \quad (5.1)$$

This equation has been used to model SANS from clusters of poly(ethylene oxide) in water.<sup>[10]</sup> The first term describes Porod scattering from the surface of the cluster. The

exponent  $n$  is predicted to be between 3 and 4 for an object with a fractal surface and will be exactly 4 if the surface is smooth.<sup>[9]</sup> The second term is a Lorentzian describing the scattering from the polymer chains. The length  $L$  is the polymer's correlation length and the exponent  $m$  is predicted to be 2 when the polymer is in a theta solvent and 1.7 for an expanded polymer in good solvent.<sup>[9]</sup>  $C_1$  and  $C_2$  are weighting factors for the two terms and  $C_3$  accounts for a constant, incoherent background.  $C_3$  was set to zero when fitting data from SGLCP solutions since incoherent background makes no apparent contribution to the scattering.

Preliminary data fitting was performed allowing all the parameters to float freely. The results gave similar values of  $n$  and  $m$  for a given polymer type (end-on or side-on) and direction (parallel or perpendicular to the director), regardless of molecular weight or temperature. A second round of data fitting was performed fixing the exponent  $m$  at its average value. The average value of  $n$  was between 2.5 and 3.2 and was therefore fixed at its theoretical minimum of 3, in agreement with the experimentally observed exponent for isotropic solutions of SGLCPs.<sup>[12, 15]</sup> The results are summarized in Table 5.2. The value of  $L$  that results when the exponents are fixed is less than 10% different from that obtained when all the parameters are floating.

$I_{par}$  from side-on polymers could not be fit with Equation 5.1 because the correlation length,  $L$ , is too large. In order to determine  $L$  from data fitting, the scattering pattern must crossover from an  $I \sim q^{-m}$  power law ( $qL \gg 1$ ) to a region approaching  $I \sim q^0$  ( $qL \ll 1$ ). When  $L$  is much larger than  $q^{-1}$  throughout the entire  $q$  range, the intensity becomes

$$I(q) = \frac{C_1}{q^n} + \frac{C_2}{L^m} q^{-m}, \quad (5.2)$$

and the value of  $L$  is absorbed into the fitting parameter  $C_2$ . Nevertheless, the fact that a crossover is not observed can be used to establish a lower bound on  $L$ . Assuming the crossover regime needs to span at least from  $q_{min} = 1.4 \times 10^{-3} \text{ \AA}^{-1}$  to  $q = 3 \times 10^{-3} \text{ \AA}^{-1}$  to be observable, the maximum value of  $L$  that can be measured with this experiment is calculated from  $qL = 3 \times 10^{-3} \text{ \AA}^{-1}$  to be 330  $\text{\AA}$ . Indeed, fixing  $m = 2$  and  $C_1 = 0$ , tabulating  $I(q)$  from Equation 5.1 at varying values of  $L$  demonstrates that an  $I \sim q^{-2}$  power law spans

the entire  $q$  range when  $L$  is larger than approximately 350 Å. The minimum value of  $L$  for side-on polymers in the direction parallel to the director is, therefore,  $\approx 350$  Å.

The correlation length in the direction perpendicular to the director,  $L_{\text{perp}}$ , is larger than  $L$  parallel to the director,  $L_{\text{par}}$ , in end-on polymer solutions (Figure 5.7a). The reverse is true for side-on polymers, where  $L_{\text{par}} > L_{\text{perp}}$  (Figure 5.7b). The conformational anisotropy, measured as the ratio of correlation lengths parallel and perpendicular to the director, is  $1.8 < L_{\text{perp}} / L_{\text{par}} < 2.1$  for both end-on polymers at 25 and 30 °C and  $L_{\text{par}} / L_{\text{perp}} > 10$  for both side-on polymers at 25 and 30 °C. The conformational anisotropy of the end-on polymers is relatively insensitive to temperature (Figure 5.7a), and the correlation lengths of both side-on and end-on polymers are systematically larger at higher molecular weight (Figure 5.7).

Although  $L_{\text{par}}$  cannot be measured for side-on polymers, their relative anisotropies from one temperature to the next can still be estimated from the SANS data and it is found that side-on polymer anisotropy is highly sensitive to temperature changes. Assuming  $C_2$  does not change significantly when the temperature is increased from 25 to 30 °C, Equation 5.2 in the high- $q$  limit where  $C_1 / q^n \approx 0$  gives the ratio of  $I_{\text{par}}$  at 25 °C to  $I_{\text{par}}$  at 30 °C:

$$\frac{I_{\text{par}}^{25^\circ\text{C}}}{I_{\text{par}}^{30^\circ\text{C}}} = \frac{C_2 / (L_{\text{par}}^{25^\circ\text{C}})^m q^{-m}}{C_2 / (L_{\text{par}}^{30^\circ\text{C}})^m q^{-m}} = \left( \frac{L_{\text{par}}^{30^\circ\text{C}}}{L_{\text{par}}^{25^\circ\text{C}}} \right)^m. \quad (5.3)$$

For 500HSiBB, the ratio is  $L_{\text{par}}^{30^\circ\text{C}} / L_{\text{par}}^{25^\circ\text{C}} = 0.55$  (Figure 5.3) and for 990HSiBB the ratio is  $L_{\text{par}}^{30^\circ\text{C}} / L_{\text{par}}^{25^\circ\text{C}} = 0.82$  (Figure 5.4). The relative changes in anisotropy,  $x = L_{\text{par}} / L_{\text{perp}}$  at 30 °C relative to that at 25 °C, may then be calculated from

$$x = \left( \frac{L_{\text{par}}^{30^\circ\text{C}}}{L_{\text{par}}^{25^\circ\text{C}}} \right) \left( \frac{L_{\text{perp}}^{25^\circ\text{C}}}{L_{\text{perp}}^{30^\circ\text{C}}} \right), \quad (5.4)$$

giving  $x = 0.53$  for 500HSiBB and  $x = 0.77$  for 990HSiBB. The anisotropy of 500HSiBB is twice as large at 25 °C as it is at 30 °C and 990HSiBB is 1.5 times as anisotropic at 25 °C as it is at 30 °C.



The correlation lengths,  $L_{iso}$ , of polymers in isotropic solution are similar regardless of whether mesogens are attached end-on or side-on (Figure 5.7). Comparing polymers with the same degree of polymerization, 350HSiCB4 and 500HSiBB both have  $L_{iso} \approx 35 \text{ \AA}$  while 760HSiCB4 and 990HSiBB both have  $L_{iso} \approx 50 \text{ \AA}$ .

## 5.4 Discussion

Solutions of 5 wt % SGLCP are found to be in the semidilute regime, evidenced by the fact that the SANS patterns are virtually independent of molecular weight and supramolecular aggregates are formed by interactions between chains. Individual polymers are indistinguishable and the characteristic length scale for scattering is the distance below which a monomer is surrounded mostly by solvent and monomers belonging to the same chain (the polymer's correlation length). Scattering from a semidilute solution does not allow the chains' overall dimensions to be measured, but the relative magnitudes of the dimensions parallel and perpendicular to the director can still be deduced because the polymer conformation inside a correlation blob is similar to the polymer's conformation in dilute solution,<sup>[8]</sup> therefore the anisotropy of the correlation lengths may be assumed the same as the anisotropy of the overall polymer chain.

Conformational anisotropy of SGLCP chains in an LC solvent derives from coupling between the orientation of the mesogenic side groups and the trajectory of the polymer backbone. Nematic interactions with the solvent cause the polymer side groups to align with the LC director, and their covalent connectivity to the backbone forces it to follow the path connecting the oriented molecules. The polymer's equilibrium conformation is determined by the thermodynamic tradeoff between the enthalpic benefit of side-group alignment and the entropic penalty of deviation from a spherical random-walk. The sense of the coupling between the side groups and the backbone, end-on or side-on, determines whether the polymer chain extends perpendicular to the director to form an oblate ellipsoid or parallel to the director to form a prolate ellipsoid.

The end-on polymers studied here have weak coupling between the side groups and the backbone, relative to that of the side-on polymers. Orienting the end-on polymer side-groups with the LC solvent results in only mild anisotropy, between 1.8 and 2.1, whereas side-on polymers have aspect ratios exceeding 10. This phenomenon may be understood by the difference in the length of the spacer separating the mesogens from the backbone. End-on side groups are separated from the polymer backbone by a ten atom spacer, whereas side-on mesogens are separated by seven atoms (Figure 5.1). End-on polymer backbones may find easier accord with the side groups' orientation field through the flexibility of a longer spacer. The inherently larger anisotropy of the side-on polymers allows the relative dimensions of the polymer to change drastically with increasing temperature as the LC solvent's orientational order decreases and the polymer approaches its spherical conformation in the isotropic phase. These changes in conformational anisotropy have a strong effect on director relaxation dynamics, as explored in detail in Chapter 6.

A notable trend is observed in the exponent  $m$  derived from fitting scattering patterns:  $m = 2.0$  for scattering in the direction parallel to the spacer connecting the side groups to the polymer backbone and  $m = 1.7$  or  $1.8$  in the direction perpendicular. This implies that the importance of excluded volume effects is anisotropic, giving some insight into the detailed molecular interactions that give rise to conformational anisotropy. Excluded volume effects appear to arise between mesogens attached adjacent to one another on the same polymer chain, causing the polymer to expand in this direction. One possible explanation is that interactions between polymer side-groups and nematic 5CB are more energetically favorable than interactions between the side-groups themselves,<sup>[8]</sup> a theory supported by the experiments discussed in Chapter 4.

Once the solutions are heated to the isotropic phase, the end-on and side-on polymers are virtually indistinguishable. The polymers adopt spherical conformations and the correlation lengths are similar at comparable molecular weights. The increased correlation length at higher molecular weight is intuitively understood because the likelihood of surrounding monomers being connected to the same chain increases with the degree of

polymerization. In the absence of nematic ordering, excluded volume effects disappear and  $m = 2.0$ , implying that favorable side-group / solvent interactions derive from nematic cross-interactions being of higher magnitude than nematic interactions in either polymer or solvent alone.

## 5.5 Conclusions

Small-angle neutron scattering from semidilute solutions of SGLCPs in a small-molecule nematic solvent reveals the conformational anisotropy of the polymer chains. The coupling between the LC solvent's orientational order and the polymer's conformation is mediated by the covalently bonded side groups. The sense (oblate or prolate) and the magnitude of the anisotropy is determined by the sense (end-on or side-on) and the magnitude of the polymer / side-group coupling: end-on polymers with weak coupling adopt mildly oblate conformations while side-on polymers with strong coupling adopt highly prolate conformations. The anisotropy of a side-on polymer is strongly dependent on temperature, but end-on polymers remain mildly oblate throughout the nematic phase. Once heated to the isotropic phase both types of polymer take on spherical conformations. The conformational anisotropy of these polymers in nematic solvent, and its temperature dependence, has a tremendous influence on the dynamics of nematic director fluctuations discussed in Chapter 6.

## 5.6 Tables

**Table 5.1** Molecular weight, conversion, and polydispersity of the side-group liquid crystal homopolymers. Details of the characterization of end-on polymers (350HSiCB4 and 760HSiCB4) may be found in Appendix A.

Name	M <sub>n</sub> (kg/mol)	Mole Fraction 1,2 PB	Mole Fraction 1,4 PB	Mole Fraction LC	PDI <sup>a</sup>
350HSiCB4	347	0	0.11	0.89	1.27
760HSiCB4	762	0.06	0.04	0.90	1.11
500HSiBB <sup>b</sup>	497	0.07	0.11	0.82	1.15
990HSiBB <sup>b</sup>	992	0.22	0.04	0.74	1.10

<sup>a</sup>PDI = Polydispersity Index ( $M_w/M_n$ )

<sup>b</sup>Synthesized and characterized by Rafael Verduzco<sup>[6]</sup>

**Table 5.2** Fitting parameters used to model scattering data with Equation 5.1

Polymer	$I_{\text{par}}$ Or $I_{\text{perp}}^a$	T [°C]	L [Å] <sup>b</sup>	m	$C_1 \times 10^7$	$C_2$
500HSiBB	$I_{\text{par}}$	25	>350	1.7	-	-
500HSiBB	$I_{\text{par}}$	30	>350	1.7	-	-
500HSiBB	$I_{\text{perp}}$	25	31.5(1)	2.0	3.6	16
500HSiBB	$I_{\text{perp}}$	30	33.5(1)	2.0	17	21
500HSiBB	-	50	33.9(1)	2.0	4.3	21
990HSiBB	$I_{\text{par}}$	25	>350	1.7	-	-
990HSiBB	$I_{\text{par}}$	30	>350	1.7	-	-
990HSiBB	$I_{\text{perp}}$	25	30.2(2)	2.0	8.1	12
990HSiBB	$I_{\text{perp}}$	30	32.0(2)	2.0	10	14
990HSiBB	-	50	47.1(4)	2.0	0.63	11
350HSiCB4	$I_{\text{par}}$	25	48.4(2)	2.0	8.2	27
350HSiCB4	$I_{\text{par}}$	30	47.7(2)	2.0	5.3	23
350HSiCB4	$I_{\text{perp}}$	25	97.7(7)	1.8	3.4	33
350HSiCB4	$I_{\text{perp}}$	30	88.0(6)	1.8	2.1	27
350HSiCB4	-	50	39.6(1)	2.0	0.077	11
760HSiCB4	$I_{\text{par}}$	25	56.9(2)	2.0	15	39
760HSiCB4	$I_{\text{par}}$	30	55.1(7)	2.0	16	4.8
760HSiCB4	$I_{\text{perp}}$	25	118(1)	1.8	4.4	48
760HSiCB4	$I_{\text{perp}}$	30	111(1)	1.8	6.5	33
760HSiCB4	-	50	49.7(3)	2.0	0.20	15

<sup>a</sup>The parallel and perpendicular designations do not apply at 50 °C, where there is no nematic director and the data are circularly averaged.

<sup>b</sup>The number in parentheses is the standard deviation in the last digit of the value of  $L$ .

## 5.7 Figures

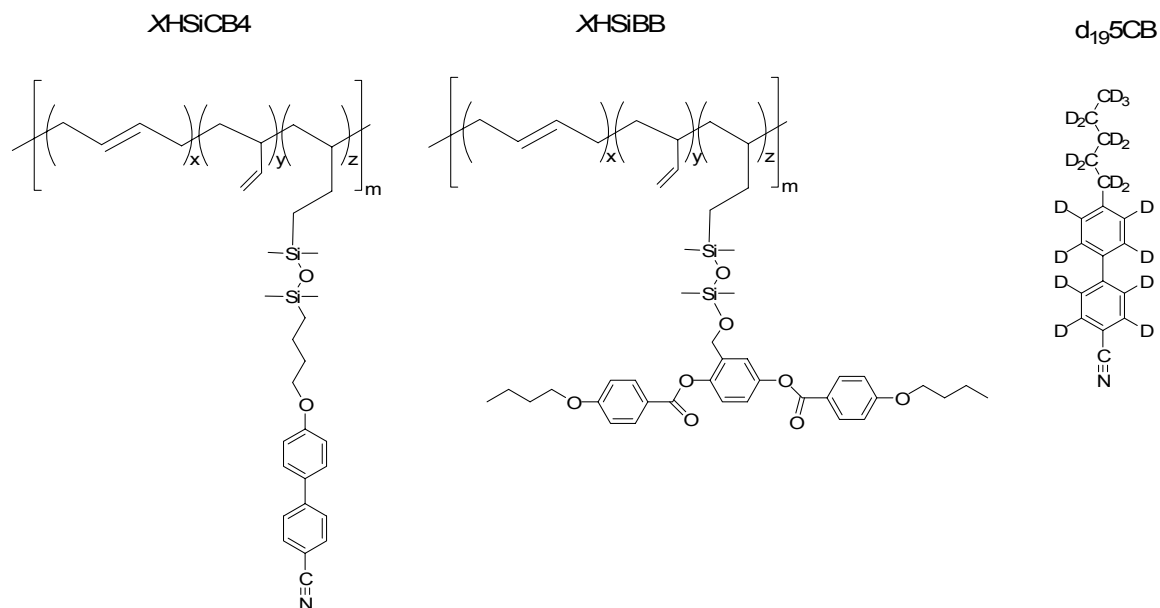


**Figure 5.1** Chemical structures of end-on (XHSiCB4) and side-on (XHSiBB) side-group liquid crystal homopolymers and the perdeuterated nematic liquid crystal solvent (d<sub>19</sub>5CB). A polymer's name is derived from its molecular weight ( $X$ ) in units of kg/mol, the letter "H" to indicate a homopolymer, and either "SiCB4" or "SiBB" to indicate either end-on or side-on mesogens, respectively. In addition to monomers having an attached mesogen, the polymer also contains some residual 1,2- and 1,4-butadiene monomers. Compositions, expressed as the mole fractions  $x$ ,  $y$ , and  $z$ , are given in Table 5.1. Details of end-on polymer characterization are presented in Appendix A, and synthesis of d<sub>19</sub>5CB is described in Appendix B.

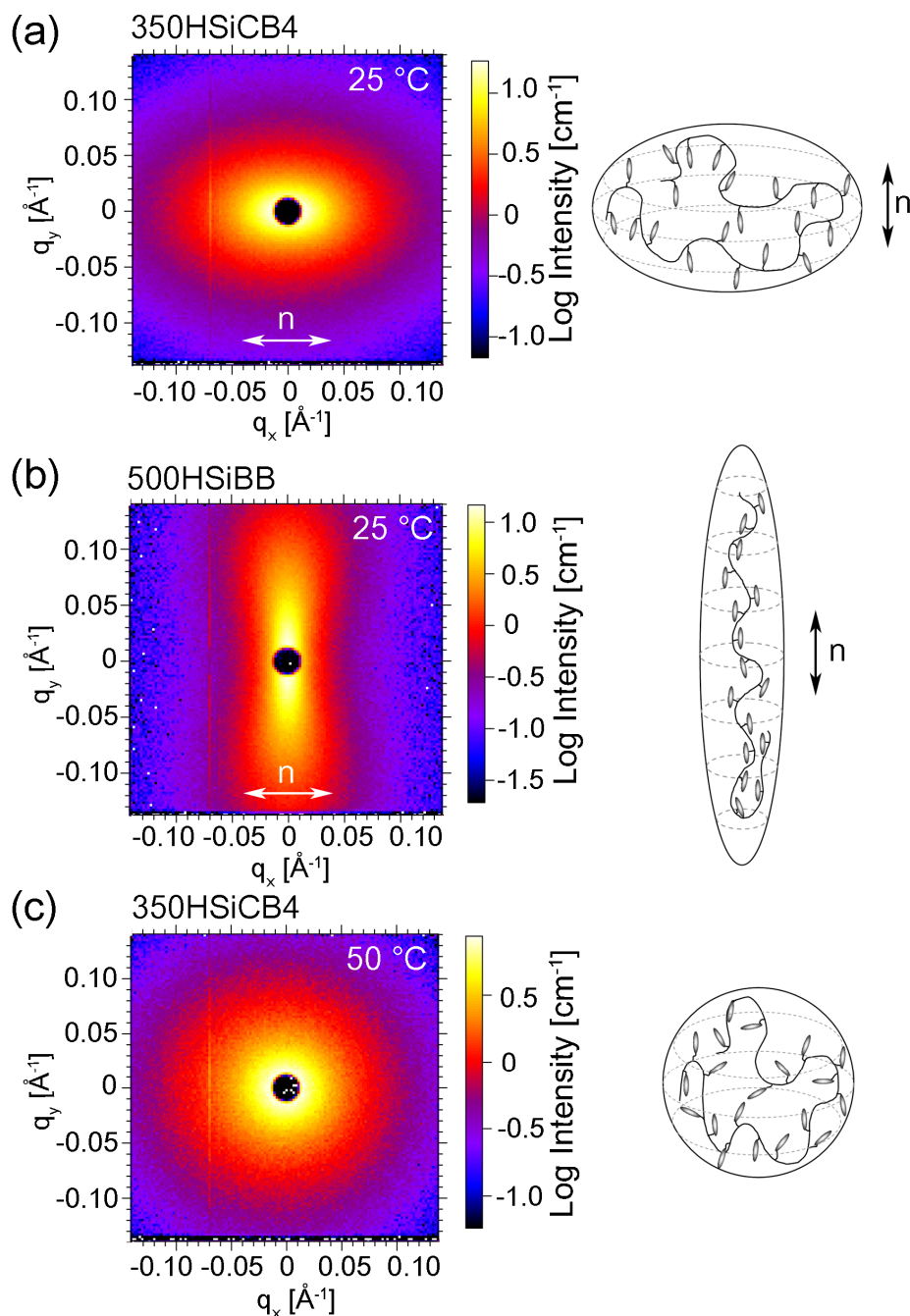


**Figure 5.2** Two-dimensional small-angle neutron scattering patterns from 5 wt % solutions of (a) oblate end-on and (b) prolate side-on homopolymers in  $d_{19}5CB$  in the nematic phase (25 °C). The orientation of the nematic director,  $n$ , is indicated by the double-headed arrows. When heated above the nematic-isotropic transition temperature, the polymers adopt a spherical conformation and the scattering patterns become circularly symmetric as illustrated with (c) end-on homopolymer solution at 50 °C.

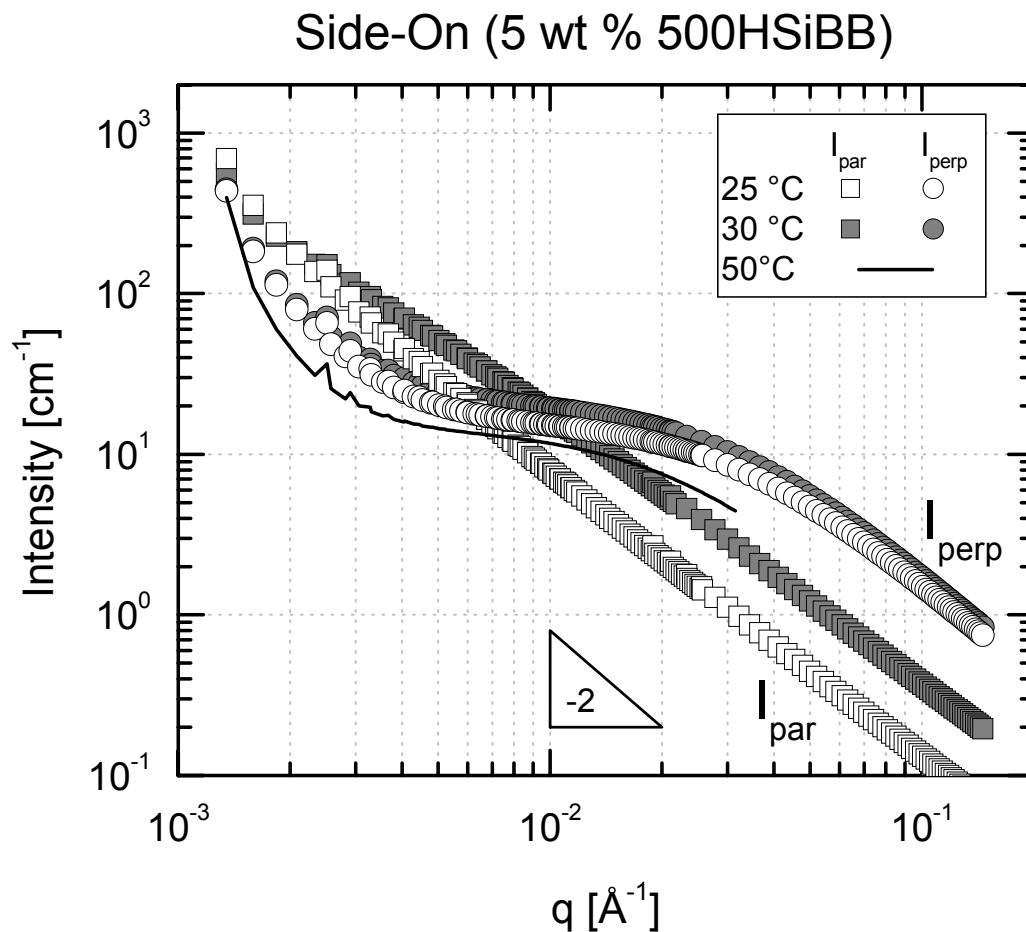


**Figure 5.3** Sector-averaged small-angle neutron scattering patterns from 5 wt % 500 HSiBB in  $d_{19}\text{5CB}$  at two temperatures in the nematic phase (25 and 30 °C) and circularly averaged scattering pattern from the sample in the isotropic phase (50 °C). “ $I_{\text{par}}$ ” and “ $I_{\text{perp}}$ ” denote sector averaging in a  $\pm 15^\circ$  wedge parallel and perpendicular to the LC director, respectively. For the sake of clarity, a solid line is used to represent data at 50 °C even though the intensity was measured at the same discrete values of  $q$  as for 25 and 30 °C data sets.



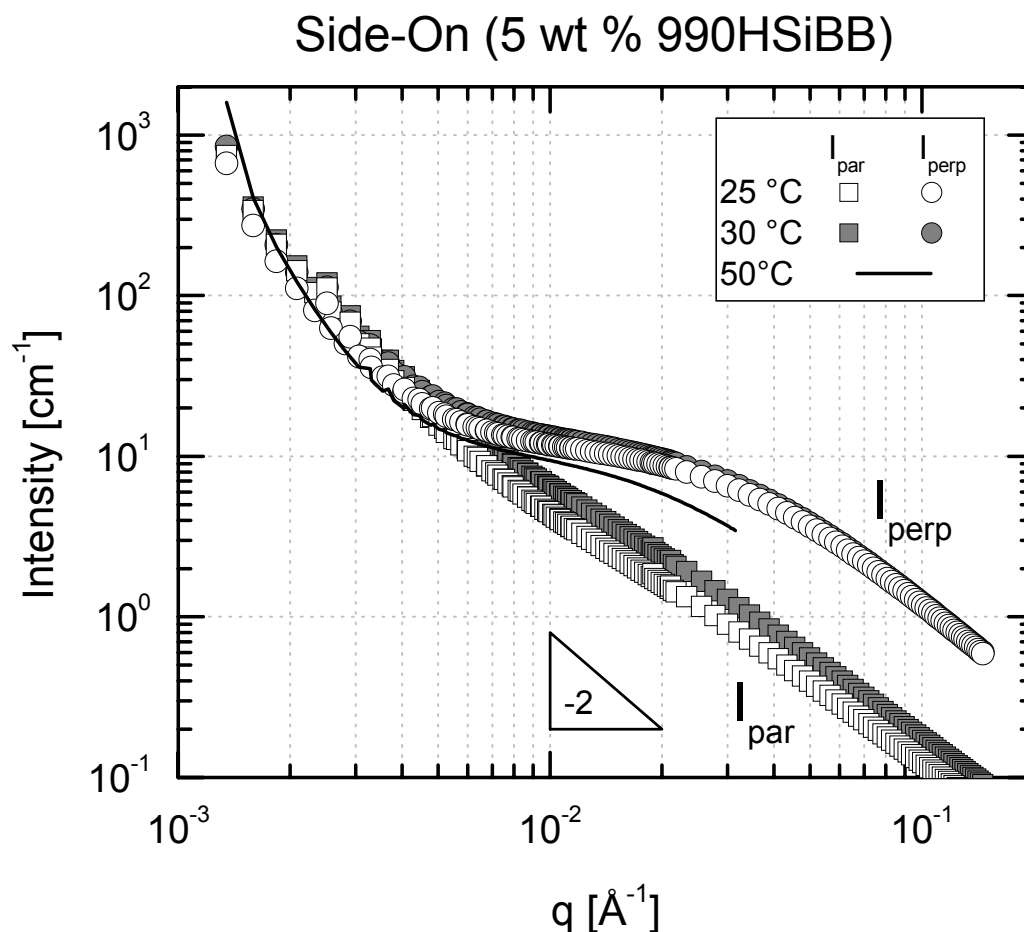


**Figure 5.4** Sector-averaged small-angle neutron scattering patterns from 5 wt % 990 HSiBB in  $d_{19}5\text{CB}$  at two temperatures in the nematic phase (25 and 30 °C) and circularly averaged scattering pattern from the sample in the isotropic phase (50 °C). “ $I_{\text{par}}$ ” and “ $I_{\text{perp}}$ ” denote sector averaging in a  $\pm 15^\circ$  wedge parallel and perpendicular to the LC director, respectively. For the sake of clarity, a solid line is used to represent data at 50 °C even though the intensity was measured at the same discrete values of  $q$  as for 25 and 30 °C data sets.

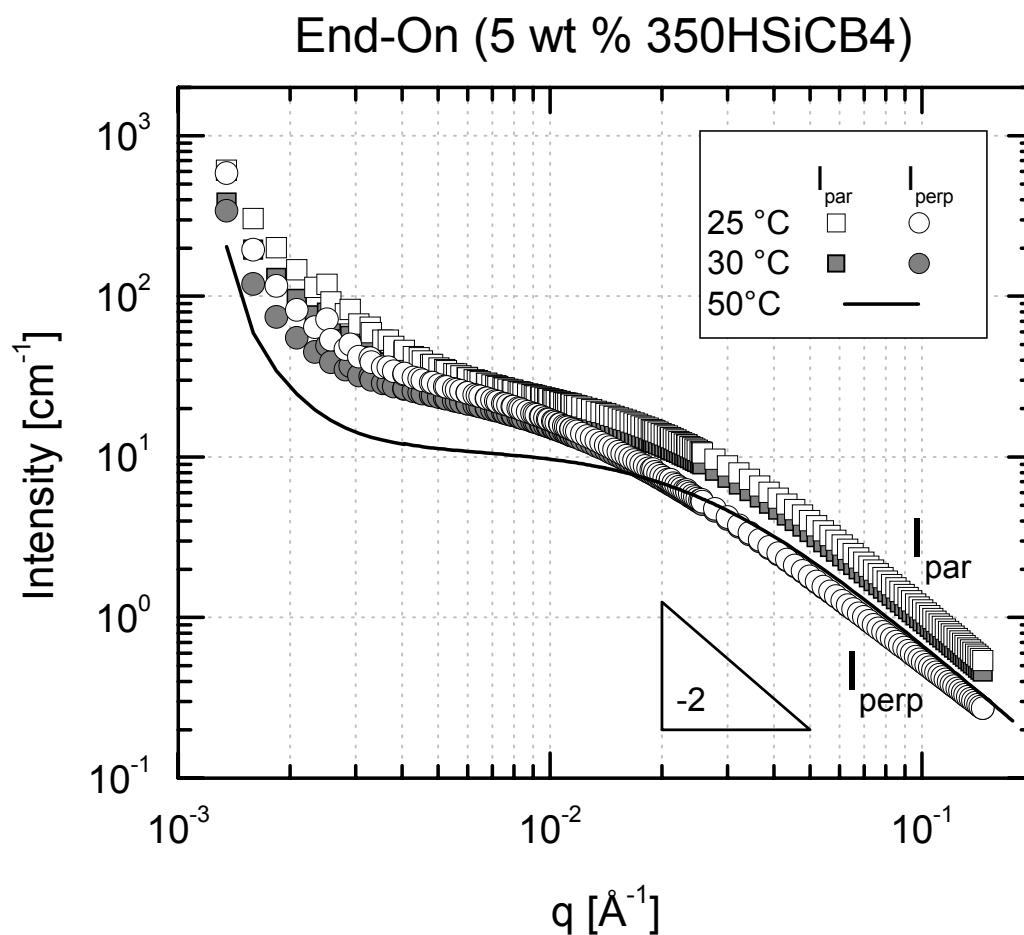


**Figure 5.5** Sector-averaged small-angle neutron scattering patterns from 5 wt % 350 HSiCB4 in d<sub>19</sub>5CB at two temperatures in the nematic phase (25 and 30 °C) and circularly averaged scattering pattern from the sample in the isotropic phase (50 °C). “ $I_{par}$ ” and “ $I_{perp}$ ” denote sector averaging in a  $\pm 15^\circ$  wedge parallel and perpendicular to the LC director, respectively. For the sake of clarity, a solid line is used to represent data at 50 °C even though the intensity was measured at the same discrete values of  $q$  as for 25 and 30 °C data sets.

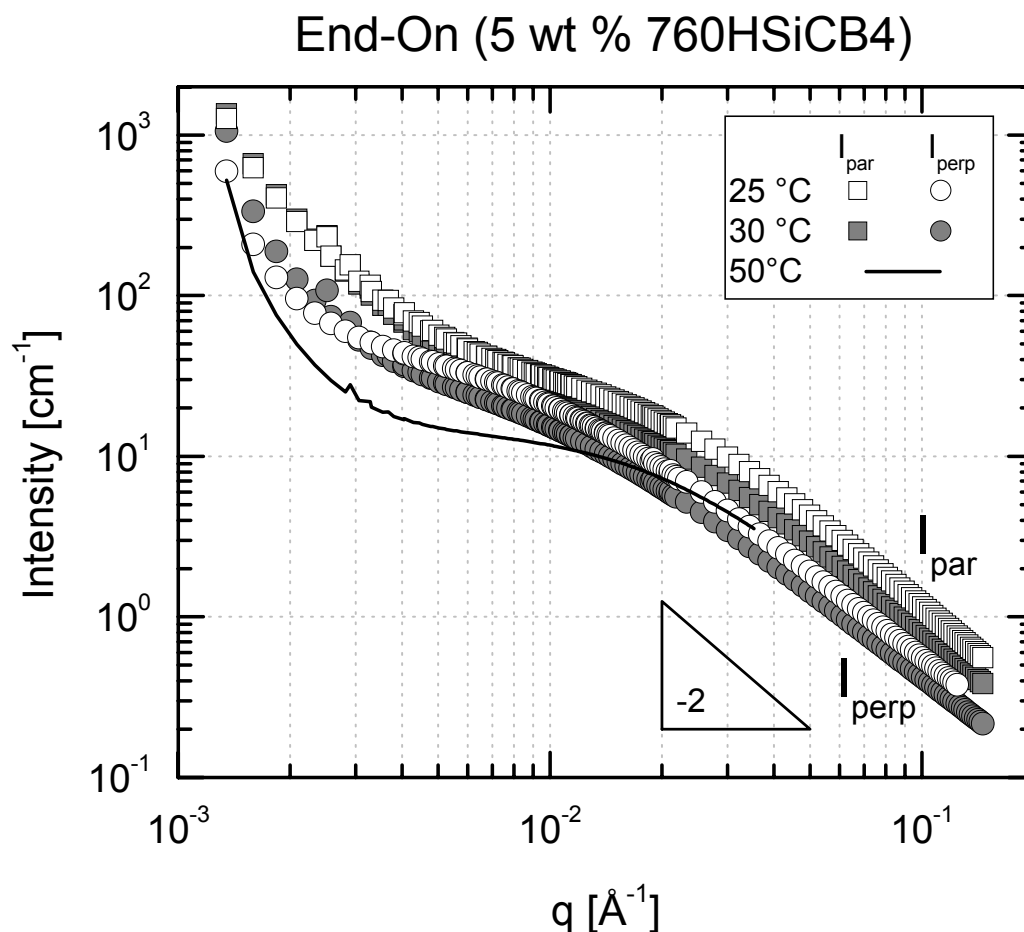


**Figure 5.6** Sector-averaged small-angle neutron scattering patterns from 5 wt % 760 HSiCB4 in  $d_{19}$ 5CB at two temperatures in the nematic phase (25 and 30 °C) and circularly averaged scattering pattern from the sample in the isotropic phase (50 °C). “ $I_{par}$ ” and “ $I_{perp}$ ” denote sector averaging in a  $\pm 15^\circ$  wedge parallel and perpendicular to the LC director, respectively. For the sake of clarity, a solid line is used to represent data at 50 °C even though the intensity was measured at the same discrete values of  $q$  as for 25 and 30 °C data sets.

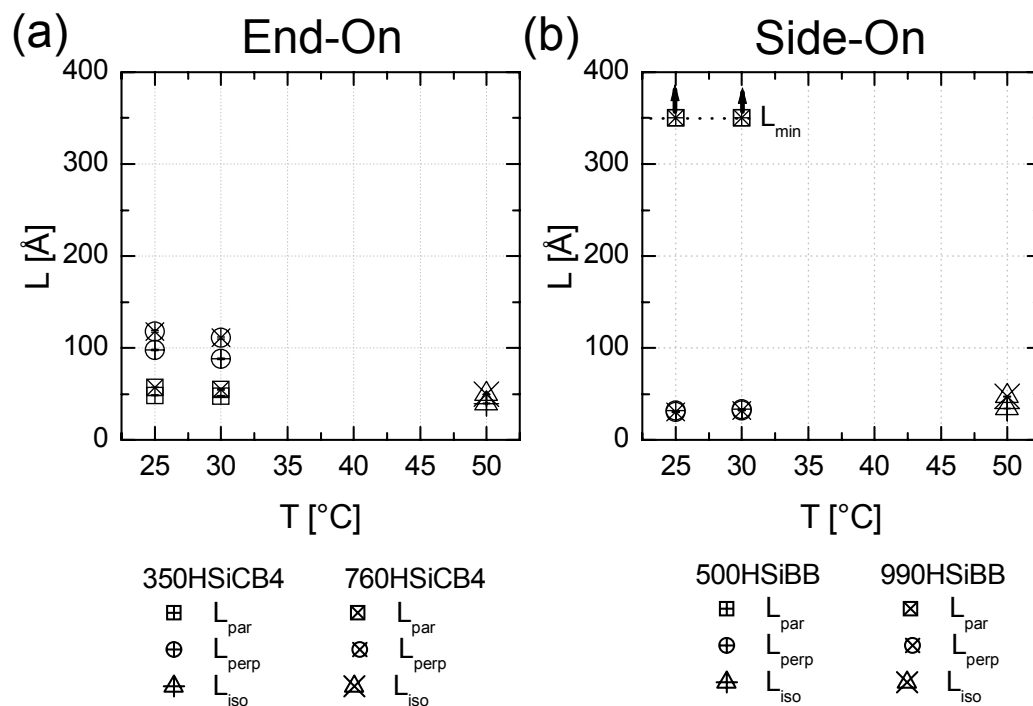


**Figure 5.7** Correlation lengths,  $L$ , in the directions perpendicular to ( $L_{perp}$ ) and parallel to ( $L_{par}$ ) the nematic director for 5 wt % solutions of (a) end-on and (b) side-on homopolymers derived from fits to scattering data using Equation 5.1. The correlation length in the isotropic phase is denoted  $L_{iso}$ . In side-on polymers,  $L_{par}$  cannot be determined by fitting, but a lower bound of  $L_{min} = 350$  Å has been established. Fitting parameters are given in Table 5.2.

## 5.8 References

- [1] Kempe, M. D.; Kornfield, J. A.; Lal, J. Chain Anisotropy Side-Group Liquid Crystalline Polymers in Nematic Solvents. *Macromolecules* **2004**, *37*, 8730-8738.
- [2] Matoussi, H.; Ober, R.; Veyssie, M.; Finkelmann, H. Conformation of Side Chain Nematic Polymers in Nematic Solutions: a Small-Angle X-Ray Scattering Study: SAXS. *Europhys. Lett.* **1986**, *2*, 233-240.
- [3] Matoussi, H.; Ober, R. Conformation of Comblike Liquid-Crystalline Macromolecules. *Macromolecules* **1990**, *23*, 1809-1816.
- [4] Carri, G. A.; Muthukumar, M. Configurations of liquid crystalline polymers in nematic solvents. *J. Chem. Phys.* **1998**, *109*, 11117-11128.
- [5] Brochard, F.; Jouffroy, J.; Levinson, P. Phase diagrams of mesomorphic mixtures. *J. Physique* **1984**, *45*, 1125-1136.
- [6] Verduzco, R. Texture Transitions, Electro-Optics, and Dynamics of Liquid Crystal Gels with Novel Network Architectures. Ph.D. Thesis, California Institute of Technology, Pasadena, CA, February 5, 2007.
- [7] Kempe, M. D.; Scruggs, N. R.; Verduzco, R.; Lal, J.; Kornfield, J. A. Self-assembled liquid-crystalline gels designed from the bottom up. *Nat. Mater.* **2004**, *3*, 177-182.
- [8] Rubinstein, M.; Colby, R. H. *Polymer Physics*, 1<sup>st</sup> ed; Oxford University Press: New York, 2003.
- [9] Higgins, J. S.; Benoit, H. C. *Polymers and Neutron Scattering*, Oxford Series on Neutron Scattering in Condensed Matter, ed. S.W. Lovesey; E.W.J. Mitchell; Oxford University Press: New York, NY, 1996.
- [10] Hammouda, B.; Ho, D. L.; Kline, S. Insight into Clustering in Poly(ethylene oxide) Solutions. *Macromolecules* **2004**, *37*, 6932-6937.
- [11] Hammouda, B.; Ho, D.; Kline, S. SANS from Poly(ethylene oxide)/Water Systems. *Macromolecules* **2002**, *35*, 8578-8585.
- [12] Richtering, W.; Gleim, W.; Burchard, W. Semidilute Solutions of Liquid Crystalline Polymers. *Macromolecules* **1992**, *25*, 3795-3801.
- [13] Viertler, K.; Wewerka, A.; Stelzer, F.; Fytas, G.; Vlassopoulos, D. Macromolecular Anisotropic Association in Isotropic Solutions of a Liquid Crystal Side Chain Polymer. *Macromol. Chem. Phys.* **2001**, *202*, 3174-3179.
- [14] Magnago, R. F.; Merlo, A. A.; Vollmer, A. F.; Mauler, R. S.; Vargas, F.; Pesco da Silveira, N. Synthesis, mesomorphic properties and light scattering of polyacrylates liquid crystals. *Polym. Bull. (Heidelberg, Ger.)* **1999**, *42*, 551-557.
- [15] Pereira, F. V.; Merlo, A. A.; Pesco da Silveira, N. Behaviour of mesogenic side group polyacrylates in dilute and semidilute regime. *Polymer* **2002**, *43*, 3901-3908.
- [16] Gallani, J. L.; Hilliou, L.; Martinoty, P. Abnormal Viscoelastic Behavior of Side-Chain Liquid-Crystal Polymers. *Phys. Rev. Lett.* **1994**, *72*, 2109-2112.